INORGANIC CHEMISTRY FRONTIERS

RESEARCH ARTICLE

View Article Online
View Journal | View Issue

Cite this: *Inorg. Chem. Front.*, 2026, **13**, 957

Acidity/hydridicity evaluation of Sb–H bonds and formation of a new group 15 metal cluster topology

Mitchell A. Z. MacEachern,[a] Tanner George [a,b] and Saurabh S. Chitnis *[a,c]

Received 15th October 2025,
Accepted 22nd November 2025

DOI: 10.1039/d5qi02115d

rsc.li/frontiers-inorganic

We report the first estimates for the proton transfer ability and hydride donor ability of a fifth-row E–H bond besides Sn–H bonds. A new D_{2d}-symmetric cluster type for M_8 species (M = pnictogen) is shown, along with the first amido-stibanide. Sterically determined deprotonation and redox outcomes are demonstrated.

The chemistry of main group element-hydrogen (E–H) bonds is an important area of study due to its relevance for synthesis (*e.g.*, reduction),[1] catalysis (*e.g.*, hydrogenation),[2] energy storage (*e.g.*, hydrogen surrogates),[3] and materials science (*e.g.*, metal deposition).[4,5] In contrast to E–H bonds involving second-, third-, and fourth-row p-block elements, the chemistry of the heavier fifth- or sixth-row elements remains underexplored due to synthetic challenges.[6,7]

The reactivity of light E–H bonds is generally well-predicted by polarity considerations.[6,7] For example, compounds containing B–H, Al–H, or Ga–H bonds generally behave as hydride sources and compounds containing N–H, P–H, or As–H bonds generally behave as proton sources. Only in rare cases, namely, when either very Lewis basic or very Lewis acidic co-reactants are present, or very strong π-donor groups flank protic E–H bonds, does the reactivity deviate from these trends.[8–10]

For heavier elements, simple bond polarity arguments are not always good predictors of reactivity as radical processes like bond homolysis can also be accessible for their long and weak E–H bonds.[6,7] This feature underpins the widespread use of light or radical-activated organotin hydrides such as $^{n}Bu_3SnH$ in organic synthesis.[11] Thus, the ability to access diverse fission pathways offers a rich bouquet of chemical reactivity for heavy main group E–H species with demonstrated practical applications. A deeper understanding of fundamental parameters for heavy E–H bonds is needed to enable the rational development of their multifaceted chemistry, but such data remain elusive. For example, widely employed acidity and hydridicity references lack values for fifth- and sixth-row main group elements (with the exception of tin), and, to the best of our knowledge, such values have not been experimentally reported for antimony or bismuth.[1,12,13] Nevertheless, species with reactive Sb–H bonds are implicated in fascinating stoichiometric and catalytic processes,[14–19] motivating the pursuit of fundamental data about this functional group and a deeper understanding of its reaction modes.

We have been studying the chemistry of Sb–H bonds in derivatives of **1RH**, starting with the discovery of hydrostibination in 2019 (Fig. 1).[20] Our original report showed that **1EtH** is a source of hydride, rapidly yielding Ph_3CH in reactions with the Ph_3C^+ cation (with presumed formation of unisolable $[\mathbf{1R}]^+$). Subsequently, we found that **1EtH** is also a source of protons towards M–N or M–C bonds, giving the first examples of bismuthanylstibanes **1RBi** and Sb–Fe bimetallics.[21,22] Finally, we found evidence of Sb–H homolysis and a radical mechanism in the reaction of **1RH** with phenylacetylene to give styrene **1RSty**.[23] Thus, derivatives of **1RH** show diverse reactivity modes within a single molecular platform. Recognizing this feature and the abovementioned scarcity of

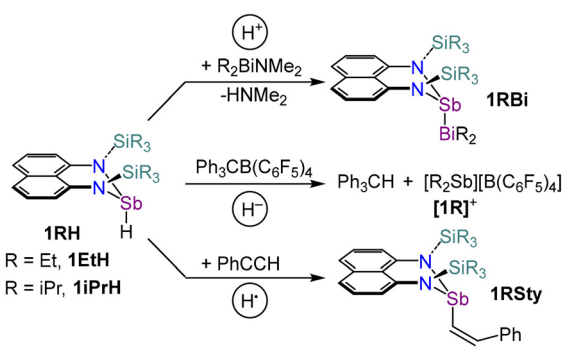

Fig. 1 Observed modes of reactivity for derivatives of **1RH**.

[a]*Department of Chemistry, Dalhousie University, Halifax, Nova Scotia, B3H 4R2, Canada. E-mail: chitnis@uvic.ca*
[b]*Department of Chemistry, Saint Mary's University, Halifax, Nova Scotia, B3H 3C3, Canada*
[c]*Department of Chemistry, University of Victoria, Victoria, British Columbia, V8P 5C2, Canada*

reactivity data for heavy E–H bonds,[24,25] here we provide the first estimates of proton and hydride transfer ability for **1RH** (R = Et, iPr) by bracketing experiments and product isolation studies. We also reveal a new main group cluster topology. Our results deepen the fundamental understanding of Sb–H bonds and metallocluster formation to guide further developments in antimony chemistry, while providing insights that may also translate to other heavy main group E–H bonds.

As compounds **1EtH** and **1iPrH** are both highly air and moisture sensitive, standard titration experiments using protic solvents are unsuitable for establishing their proton transfer ability. Moreover, as we show later, the anions formed by deprotonation only have a fleeting existence, precluding the establishment of a true equilibrium between the derivatives of **1RH**, H^+, and $[1R]^-$. Given these limitations, we adopted a bracketing approach involving the combination of **1RH** with organic bases whose pK_a values are known in THF to look for evidence of proton transfer. The pK_a of the most basic species that fails to react with **1RH** forms one limit of the pK_a bracket, while the pK_a of the least basic species that deprotonates **1RH** forms the other limit. An additional limitation arises from the possibility of base coordination to the metal rather than deprotonation as we have previously shown the derivatives of **1RH** exhibit antimony-centred Lewis acidity and coordination.[20,23] To thwart such coordination and promote reactivity at the Sb–H bond, only bases of moderate to high steric bulk that were soluble in non-protic solvents were suitable.

Through pairwise reactions between equimolar amounts of **1EtH** and >20 bases, we successively narrowed the limits of the pK_a range spanned by the limiting bases. This process culminated with the finding that piperidine (pK_a of conjugated acid in THF = 14.3)[26] failed to deprotonate **1EtH** while 1,1,3,3-tetramethylguanidine (TMG, pK_a of conjugated acid in THF = 15.5)[26] succeeded, bracketing the proton transfer ability of **1EtH** to within the 14.3–15.5 pK_a range in THF (Fig. S1–S5). No other suitable base could be found within this range to further narrow the pK_a bracket. The analogous sequence of experiments with **1iPrH** indicated a proton transfer ability value in the 20.2–21.0 pK_a range, with the phosphazene base ^{t}butylimino-tri(pyrrolidino)phosphorane (BTTP, pK_a of conjugate acid in THF = 20.2)[26] being unable to significantly deprotonate this compound, while 7-methyl-1,5,7-trizabicyclodecene (TBD, pK_a of conjugate acid in THF = 21.0)[26] was successful (Fig. S6–S9). To the best of our knowledge, despite being ranges rather than absolute values, these represent the first experimental acidity measurements for any fifth- or sixth-row main group E–H bond, besides Sn–H bonds.

The significant reduction in acidity going from **1EtH** to **1iPrH** was surprising, given that the Sb–H group is well-separated from the substitutional changes occurring in the silyl groups. We hypothesized that this may have a kinetic origin, namely, that the bulky triisopropylsilyl groups prevent approach of the base to the Sb–H bond, thereby suppressing deprotonation that may otherwise readily occur in a less hindered case. To evaluate this possibility, we calculated the energies for transferring a proton from each compound to the diisopropylamide anion using density functional theory and a polarization continuum model for THF. The ΔG for this reaction (−34.07 kcal mol^{-1}) captures the relative acidity of **1EtH** and iPr_2NH, indicating that the latter is 24.99 pK_a units less acidic than the former. Based on the experimentally known pK_a of iPr_2NH (35.7 in THF), a DFT-calculated value of 10.71 is obtained for **1EtH**.[27] The analogous calculation for **1iPrH** yielded a calculated pK_a of 9.06. These calculated values, which reflect thermodynamic, not kinetic, outcomes by ignoring counterion, solvation, and steric effects, are quite close to one another (within 2 pK_a units). By comparison, the experimental brackets for the two compounds are separated by almost 6 pK_a units, supporting our hypothesis of kinetic inhibition for **1iPrH**.

Next, we sought to isolate the stibanide anions resulting from deprotonation of **1RH**. Breunig has previously characterized derivatives of $R_2SbLi(THF)_3$ (R = Ph, Mes; Mes = 2,4,6-trimethylphenyl) by deprotonation of the corresponding R_2SbH precursor with nBuLi in THF.[28] Power also generated the Ph_2Sb^- anion in a crown ether solvated lithium salt *via* deprotonation of Ph_2SbH with nBuLi.[29] More recently, von Hänisch isolated alkali metal salts of the parent stibanide, $[SbH_2]^-$, *via* reaction between SbH_3 and nBuLi or MO^tBu salts (M = Na, K, Rb, Cs).[30] In contrast to such compounds, derivatives of **1RH** feature π-electron-rich amido groups and stibanides featuring such groups remain unknown, further motivating our attempts to isolate them.

Combining **1EtH** with LiHMDS resulted in an immediate colour change to dark red/orange and formation of hexamethyldisilazane, as per ^{1}H NMR spectroscopy. The prominent ^{1}H NMR resonance of the Sb–H group at *ca.* 10 ppm also disappeared, as did the associated Sb–H stretch at 1883 cm^{-1} in the IR spectrum (Fig. S20). Storage of the solution at −30 °C yielded red crystals identified by a diffraction experiment as compound **2**, which has the overall formula $(LSb\text{-}Sb)_4$, where L is the triethylsilyl naphthalenediamine ligand (Fig. 2). This outcome confirms the deprotonation but indicates that the subsequent anion is unstable towards redox rearrangement and ligand loss, instead yielding polystibanes. Such redox chemistry has previously only been observed in reactions of antimony centres containing a single organic group [*e.g.* $RSbCl_2$ or *cyclo*-$(RSb)_n$] and reducing agents such as alkali

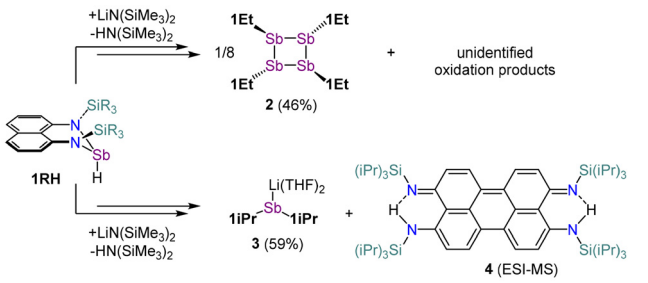

Fig. 2 Formation of compounds **2** and **3** and oxidation product **4** detected by ESI-MS.

metals.[28,31] Cluster formation has, however, not been observed following deprotonation of Ar_2SbH or SbH_3,[30] highlighting the distinct reactivity of amido-substituted secondary stibanes. It is likely that the increased lability of the very polar Sb–N bonds compared to Sb–C or Sb–H bonds permits reaction trajectories involving the loss of even chelating amido ligands. The electron-rich nature of the naphthalenediamine ligand also makes it more susceptible to oxidation.[32–34]

The structure of compound **2** is remarkable for two reasons. First, the open D_{2d}-symmetric metal core (Fig. 3b) is unprecedented for pnictogens. Reported molecular Sb_8 compounds form S_8-like eight-membered rings,[35] realgar-like closed polycycles,[36] or interconnected 2 × Sb_4 rings.[37] Second, the planarity of the Sb_4 core (D_{4h}) is unexpected in the absence of any obvious multiple bonding. Indeed, four-membered pnictogen rings form folded structures (Fig. 3c), whereas the Sb_4 core of **2** is more reminiscent of σ-aromatic $[M_4]^{4+}$ rings.[38]

Multiple bonding can be ruled out as the cause of planarity since the Sb–Sb bond distances within the Sb_4 core [2.8452(4)–2.8683(4) Å] are comparable to those between the core and peripheral Sb atoms [2.8264(4)–2.8342(4) Å]. Lattice packing effects can also be discounted since the DFT-calculated structure of an isolated molecule closely resembles the one that is experimentally observed. And although we have previously shown that silylnaphthalene diamine ligands are exceptional dispersion donors,[39] this feature appears to have only a minor effect in terms of promoting planarity – DFT calculations including or omitting dispersion corrections gave very similar geometries, matching the experimental structure (Fig. S23). Instead, it appears that the high steric repulsion between the silyl groups forces the ring to be flat such that the distance between the ligands is maximized. Consistently, the only other molecule showing such an open D_{2d} M_8 arrangement (M = main group metal) is $[(Me_3Si)_3Ge–Ge]_4$, which features the very large $(Me_3Si)_3Ge$ group.[40] Further supporting this steric repulsion argument, the DFT-optimized geometry of a hypothetical, sterically *unhindered*, N–Me substituted derivative showed a heavily puckered ring (metal portion shown in Fig. 3c, see Fig. S22) that reflects the expected shape for such a species.

The analogous anion isolation experiment of **1iPrH** with LiHMDS also showed complete loss of the Sb–H functional group by NMR and IR spectroscopy. However, recrystallization of the reaction mixture in this case gave a lithium tristibanide salt **3** as a THF solvate (Fig. 3d). Tristibanides have previously been prepared by reduction of cyclotetrastibanes or triarylstibanes with alkali metals.[29,41] Formation of an Sb_3 rather than Sb_8 unit from **1iPrH** is likely due to the high steric bulk of the triisopropylsilyl groups, which prevents the more extensive aggregation needed to make the Sb_8 cluster found in **2**. In this context, compound **3** can be considered a kinetic snapshot of a stabilized intermediate en route to larger clusters. The Sb–Sb bond distances in the tristibanide **3** [2.7704(9) and 2.7546(8) Å] are on average 0.07 Å shorter than the corresponding values in the neutral polystibane **2**, while the average Sb–N distance in **3** (2.083 Å) is slightly longer than in **2** (2.042 Å). We ascribe these differences to hyperconjugation between the lone pairs at Sb2 and the Sb1–N σ* acceptor orbitals, which would increase Sb2–Sb1 covalency at the expense of Sb1/3-N bonding.

To determine the fate of the lost ligand equivalents in formation of **2** and **3**, we conducted mass spectrometric analyses of reaction mixtures from which these clusters were obtained (Fig. S24–S30). The spectra for the reaction involving **1iPrH** showed formation of tetraaminoperylene **4** (Fig. S28), which is the expected oxidation product in line with Gade's previous report that 1,8-bis(silylamino)naphthalene complexes of thallium (a fifth-row metal like antimony) undergo loss of reduced thallium metal with concomitant formation of tetraaminoperylenes.[32]

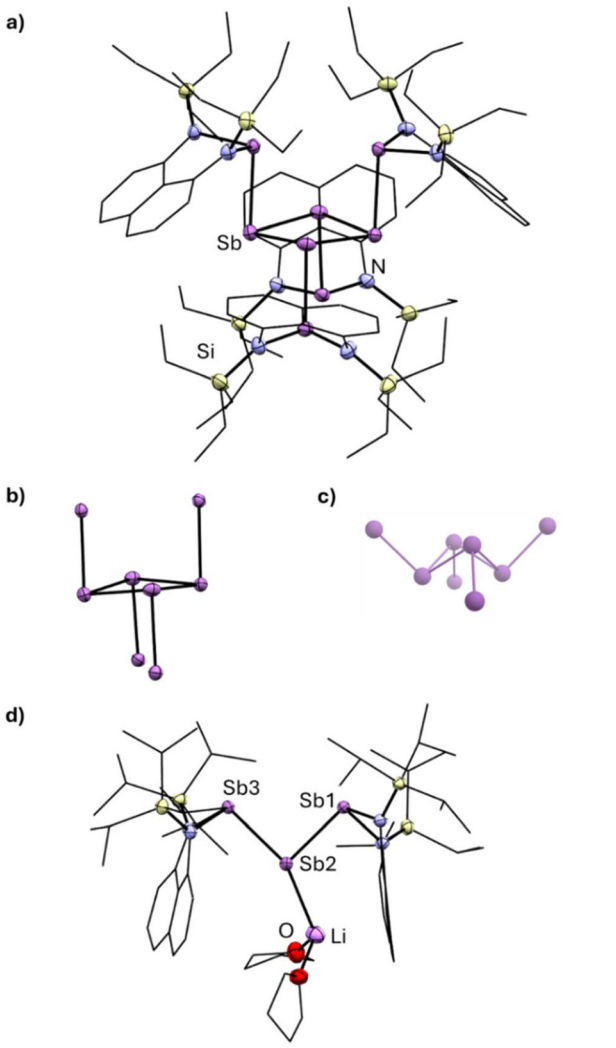

Fig. 3 (a) Structure of **2** in the solid state as determined by single crystal diffraction. Hydrogen atoms have been omitted, and ellipsoids are drawn at 50% probability. (b) The Sb_8 core of compound **2** with amido ligands omitted for clarity. (c) The folded structure of the Sb_8 core, as found in the calculated structure of N–Me substituted derivative **2'**. (d) Structure of **3** in the solid state as determined by single crystal diffraction. Hydrogen atoms have been omitted, and ellipsoids are drawn at 50% probability. Lithium aryl interactions are omitted but are comprised by an η^4 interaction with the naphthalene ring.

To estimate the hydride ion affinity of $[\mathbf{1R}]^+$, a similar bracketing methodology was applied. After testing >20 boron, carbon, and silicon-based Lewis acids, we observed that (i) boron Lewis acids were unsuitable due to formation of multiple B–C/Sb–H metathesis products, and (ii) both stibanes readily transferred a hydride to the $[Ph_3C]^+$ cation (calculated hydride ion affinity = 471.5 kJ mol^{-1} in dichlorobenzene).[42] The latter reactions result in the clean disappearance of the Sb–H resonance and appearance of the C–H resonance of triphenylmethane. Moreover, we found that neither stibane transferred a hydride to the $[Et_3Si]^+$ cation (calculated hydride ion affinity = 463.6 kJ mol^{-1} in dichlorobenzene).[42] This allows us to bracket the hydride ion affinity of $[\mathbf{1R}]^+$ as being in the 463.6–471.5 kJ mol^{-1} range, which almost perfectly encapsulates the DFT-calculated HIA values of 461 kJ mol^{-1} for **1EtH** and 460 kJ mol^{-1} for **1iPrH**, indicating minimal steric modulation. Diarylstibenium cations have previously been prepared by hydride abstraction from secondary stibanes.[43,44] N-heterocyclic stibenium ions, including those featuring a naphthalenediamine core, have been structurally authenticated previously.[45–48] However, several attempts showed that isolation of these highly reactive cations with N-silyl ligands was not possible in our hands. Once generated, they decomposed with half-lives on the order of hours in solvent, precluding access to pure samples. Crystallization attempts gave oils that continued to degrade even under inert atmosphere. Nevertheless, in line with the bracketing above, we confirmed that addition of Et_3SiH to the putative $[\mathbf{1R}]^+$ product in the reaction between **1RH** and $[Ph_3C]^+$ immediately regenerated the resonances for **1RH** (Fig. S10–S13), supporting the intermediacy of a stibenium ion abstracting hydride from Et_3SiH.

In summary, we have determined the first estimates for the proton transfer ability and hydride donor ability of two stibanes, providing rare fundamental data about fifth-row E–H bonds. The proton transfer ability estimates reflect effective acidity rather than absolute acidity because true equilibrium between **1RH** and $[\mathbf{1R}]^-$ is prevented by the onward redox reactivity of the stibanides to give clusters and chains. Nevertheless, observations employing a broad range of bases reproducibly and unambiguously indicate that diamidostibanes are comparable in acidity to protonated guanidines (pK_a ~15), except when sterically very hindered. The latter point is made by **1iPrH**, which shows comparably low acidity to protonated phosphazene superbases (pK_a ~20). As part of attempts to isolate stable stibanides, we additionally isolated the first D_{2d}-symmetric M_8 cluster for the pnictogens, evidencing a topology that has only been observed in the case of one germanium species.[40] The first amido-substituted tristibanide was also isolated. The isolation of these clusters evidences divergent behaviour towards bases as a function of substituent at Sb (aryl *vs.* amido), and steric bulk ($NSiEt_3$ *vs.* $NSi(^iPr)_3$). On the other end of the spectrum, bracketing experiments indicate that the stibanes are slightly weaker hydride donors (HIA ~460 kJ mol^{-1}) than trialkylsilanes like Et_3SiH. Here, the stibenium products could not be isolated due to instability, but strong evidence of their formation and persistence was observed by reverse titration with Et_3SiH. Collectively, these results provide insights into Sb–H bonds, which may have implications for future applications in areas such as catalysis, main group nanocluster formation, and metal deposition.

Conflicts of interest

There are no conflicts to declare.

Data availability

The data supporting this article have been included as part of the supplementary information (SI). Supplementary information is available. See DOI: **https://doi.org/10.1039/d5qi02115d**.

CCDC 2495433 (**2**) and 2495434 (**3**) contain the supplementary crystallographic data for this paper.[49a,b]

References

1 Z. M. Heiden and A. P. Lathem, Establishing the Hydride Donor Abilities of Main Group Hydrides, *Organometallics*, 2015, **34**, 1818–1827.
2 H. Yu, X. Li and J. Zheng, Beyond Hydrogen Storage: Metal Hydrides for Catalysis, *ACS Catal.*, 2024, **14**, 3139–3157.
3 N. Klopčič, I. Grimmer, F. Winkler, M. Sartory and A. Trattner, A review on metal hydride materials for hydrogen storage, *J. Energy Storage*, 2023, **72**, 108456.
4 K. J. Blakeney and C. H. Winter, Atomic Layer Deposition of Aluminum Metal Films Using a Thermally Stable Aluminum Hydride Reducing Agent, *Chem. Mater.*, 2018, **30**, 1844–1848.
5 H. Nagayoshi, S. Nishimura, T. Takeuchi, M. Hirai and K. Terashima, GaN growth using gallium hydride generated by hydrogenation of liquid gallium, *J. Cryst. Growth*, 2005, **275**, e1007–e1010.
6 M. M. D. Roy, A. A. Omaña, A. S. S. Wilson, M. S. Hill, S. Aldridge and E. Rivard, Molecular Main Group Metal Hydrides, *Chem. Rev.*, 2021, **121**, 12784–12965.
7 S. Aldridge and A. J. Downs, Hydrides of the Main-Group Metals: New Variations on an Old Theme, *Chem. Rev.*, 2001, **101**, 3305–3366.
8 L. Wu, S. S. Chitnis, H. Jiao, V. T. Annibale and I. Manners, Non-Metal-Catalyzed Heterodehydrocoupling of Phosphines and Hydrosilanes: Mechanistic Studies of $B(C_6F_5)_3$-Mediated Formation of P-Si Bonds, *J. Am. Chem. Soc.*, 2017, **139**, 16780–16790.
9 T. Kaese, H. Budy, M. Bolte, H.-W. Lerner and M. Wagner, Deprotonation of a Seemingly Hydridic Diborane(6) To Build a B–B Bond, *Angew. Chem., Int. Ed.*, 2017, **56**, 7546–7550.
10 D. Gudat, A. Haghverdi, T. Gans-Eichler and M. Nieger, High stability of a phosphenium ion allows Umpolung of

P-H bonds, *Phosphorus, Sulfur Silicon Relat. Elem.*, 2002, **177**, 1637–1640.
11 A. G. Davies, Recent Advances in the Chemistry of the Organotin Hydrides, *J. Chem. Res.*, 2006, **2006**, 141–148.
12 F. G. Bordwell, Equilibrium acidities in dimethyl sulfoxide solution, *Acc. Chem. Res.*, 1988, **21**, 456–463.
13 M. Horn, L. H. Schappele, G. Lang-Wittkowski, H. Mayr and A. R. Ofial, Towards a Comprehensive Hydride Donor Ability Scale, *Chem. – Eur. J.*, 2013, **19**, 249–263.
14 P. Novák, M. Erben, R. Jambor, M. Hejda, A. Růžička, E. Rychagova, S. Ketkov and L. Dostál, The reactivity of antimony and bismuth N,C,N-pincer compounds toward K[BEt3H] – the formation of heterocyclic compounds vs. element–element bonds vs. stable terminal Sb–H bonds, *Dalton Trans.*, 2023, **52**, 218–227.
15 C. Helling, C. Wolper and S. Schulz, Synthesis of heteroleptic gallium-substituted antimony hydrides by stepwise beta-H elimination, *Dalton Trans.*, 2020, **49**, 11835–11842.
16 R. J. Baker, M. Brym, C. Jones and M. Waugh, 9-Triptycenyl complexes of group 13 and 15 halides and hydrides, *J. Organomet. Chem.*, 2004, **689**, 781–790.
17 H. Breunig and J. Probst, Reactions of Ph_2SbH and p-TolSbH(2) with organic compounds, *J. Organomet. Chem.*, 1998, **571**, 297–303.
18 M. Huang, K. Li, Z. Zhang and J. Zhou, Antimony Redox Catalysis: Hydroboration of Disulfides through Unique Sb(I)/Sb(III) Redox Cycling, *J. Am. Chem. Soc.*, 2024, **146**, 20432–20438.
19 Y. Pang, M. Leutzsch, N. Nöthling and J. Cornella, Dihydrogen and Ethylene Activation by a Sterically Distorted Distibene, *Angew. Chem., Int. Ed.*, 2023, **62**, e202302071.
20 K. M. Marczenko, J. A. Zurakowski, K. L. Bamford, J. W. M. MacMillan and S. S. Chitnis, Hydrostibination, *Angew. Chem., Int. Ed.*, 2019, **58**, 18096–18101.
21 K. M. Marczenko and S. S. Chitnis, Bismuthanylstibanes, *Chem. Commun.*, 2020, **56**, 8015–8018.
22 J. A. Zurakowski, M. A. Z. MacEachern, C. S. Durfy, P. D. Boyle, S. S. Chitnis and M. W. Drover, Hydro- and chloroelementation reactions across an iron–carbon bond using heavy group 15 reagents, *Chem. Commun.*, 2025, **61**, 10969–10972.
23 J. W. M. MacMillan, K. M. Marczenko, E. R. Johnson and S. S. Chitnis, Hydrostibination of Alkynes: A Radical Mechanism*, *Chem. – Eur. J.*, 2020, **26**, 17134–17142.
24 M. Wiesemann, M. Niemann, J. Klösener, B. Neumann, H.-G. Stammler and B. Hoge, Tris(pentafluoroethyl)stannane: Tin Hydride Chemistry with an Electron-Deficient Stannane, *Chem. – Eur. J.*, 2018, **24**, 2699–2708.
25 M. Wiesemann, J. Klösener, M. Niemann, B. Neumann, H.-G. Stammler and B. Hoge, The Tris(pentafluoroethyl)stannate(II) Anion, $[Sn(C_2F_5)_3]^-$—Synthesis and Reactivity, *Chem. – Eur. J.*, 2017, **23**, 14476–14484.
26 S. Tshepelevitsh, A. Kütt, M. Lõkov, I. Kaljurand, J. Saame, A. Heering, P. G. Plieger, R. Vianello and I. Leito, On the Basicity of Organic Bases in Different Media, *Eur. J. Org. Chem.*, 2019, 6735–6748.
27 Note that the discrepancy between the calculated and experimental value for **1EtH** (observed bracket 14.3–15.5, calculated 9.06) is unsurprising since explicit solvation and counterion effects are not considered in the DFT calculation.
28 H. Breunig, M. Ghesner and E. Lork, Syntheses of the antimonides R_2Sb^- (R = Ph, Mes, tBu, tBu_2Sb) and $Sb_7^{(3-)}$ by reactions of organoantimony hydrides or cyclo-$(tBuSb)_{(4)}$ with Li, Na, K, or BuLi, *Z. Anorg. Allg. Chem.*, 2005, **631**, 851–856.
29 R. A. Bartlett, H. V. Rasika Dias, H. Hope, B. D. Murray, M. M. Olmstead and P. P. Power, Isolation and structural characterization of the solvated lithium salts of the Group VA (15) anions $[EPh_2]^-$ (E = nitrogen, phosphorus, arsenic or antimony) and $[Sb_3Ph_4]$, *J. Am. Chem. Soc.*, 1986, **108**, 6921–6926.
30 K. Dollberg, S. Schneider, R.-M. Richter, T. Dunaj and C. von Hänisch, Synthesis and Application of Alkali Metal Antimonide—A New Approach to Antimony Chemistry, *Angew. Chem., Int. Ed.*, 2022, **61**, e202213098.
31 H. Breunig and R. Rosler, Organoantimony compounds with element-element bonds, *Coord. Chem. Rev.*, 1997, **163**, 33–53.
32 L. H. Gade, C. H. Galka, K. W. Hellmann, R. M. Williams, L. De Cola, I. J. Scowen and M. McPartlin, Tetraaminoperylenes: Their Efficient Synthesis and Physical Properties, *Chem. – Eur. J.*, 2002, **8**, 3732–3746.
33 C. H. Galka, D. J. M. Troesch, I. Ruedenauer, L. H. Gade, I. Scowen and M. McPartlin, Synthesis and Structural Characterization of Metalated 1,8-Bis(silylamino)naphthalene Derivatives, *Inorg. Chem.*, 2000, **39**, 4615–4620.
34 K. W. Hellmann, C. Galka, L. H. Gade, A. Steiner, D. S. Wright, T. Kottke and D. Stalke, Aggregation of lithium and mixed thallium(I)-lithium amides through η3- and η6-π-arene interactions in the solid, *Chem. Commun.*, 1998, 549–550, DOI: **10.1039/a708139a**.
35 Y.-H. Xu, W.-J. Tian, J.-Y. Sun, M. Scheer and Z.-M. Sun, Extension and Fusion of Cyclic Polyantimony Units, *J. Am. Chem. Soc.*, 2024, **146**, 15473–15478.
36 L. Balázs and H. Breunig, Organometallic compounds with Sb-Sb or Bi-Bi bonds, *Coord. Chem. Rev.*, 2004, **248**, 603–621.
37 G. Balázs, H. J. Breunig, E. Lork and S. Mason, Neutron Diffraction Crystallography of meso-R(H)Sb–Sb(H)R and Reactions of R(H)Sb–Sb(H)R and $RSbH_2$ (R = $(Me_3Si)_2CH$) Leading to Tungsten Carbonyl Complexes, Methylstibanes, and Antimony Homocycles, *Organometallics*, 2003, **22**, 576–585.
38 R. Yadav, A. Maiti, M. Schorpp, J. Graf, F. Weigend and L. Greb, Supramolecular trapping of a cationic all-metal σ-aromatic $\{Bi_4\}$ ring, *Nat. Chem.*, 2024, **16**, 1523–1530.
39 N. J. Roberts, E. R. Johnson and S. S. Chitnis, Dispersion Stabilizes Metal–Metal Bonds in the 1,8-Bis(silylamido)

naphthalene Ligand Environment, *Organometallics*, 2022, **41**, 2180–2187.

40 S. P. Mallela, S. Hill and R. A. Geanangel, New Small-Ring Cyclogermanes: Syntheses and X-ray Crystal Structures, *Inorg. Chem.*, 1997, **36**, 6247–6250.

41 H. Althaus, H. J. Breunig, J. Probst, R. Rösler and E. Lork, The crystal structure of a trinuclear anion, $[(t\text{-}Bu_2Sb)_2Sb]^-$ formed by reaction of cyclo-$(t\text{-}Bu_4Sb_4)$ with potassium, and the four-membered rings, cyclo-$(t\text{-}Bu_4EnSb_{4\text{-}n})$ (E=P, n=0–3; E=As, n=0–2), *J. Organomet. Chem.*, 1999, **585**, 285–289.

42 D. G. Gusev and O. V. Ozerov, Calculated Hydride and Fluoride Affinities of a Series of Carbenium and Silylium Cations in the Gas Phase and in C_6H_5Cl Solution, *Chem. – Eur. J.*, 2011, **17**, 634–640.

43 M. Olaru, D. Duvinage, E. Lork, S. Mebs and J. Beckmann, Transient Phosphenium and Arsenium Ions versus Stable Stibenium and Bismuthenium Ions, *Chem. – Eur. J.*, 2019, **25**, 14758–14761.

44 M. Olaru, D. Duvinage, E. Lork, S. Mebs and J. Beckmann, Heavy Carbene Analogs: Donor-Free Bismuthenium and Stibenium Ions, *Angew. Chem., Int. Ed.*, 2018, **57**, 10080–10084.

45 H. A. Spinney, I. Korobkov, G. A. DiLabio, G. P. A. Yap and D. S. Richeson, Diamidonaphthalene-Stabilized N-Heterocyclic Pnictogenium Cations and Their Cation–Cation Solid-State Interactions, *Organometallics*, 2007, **26**, 4972–4982.

46 N. Sen, P. Gothe, P. Sarkar, S. Das, S. Tothadi, S. K. Pati and S. Khan, Donor free stibenium cation as an efficient cyanosilylation catalyst, *Chem. Commun.*, 2022, **58**, 10380–10383.

47 T. Gans-Eichler, D. Gudat and M. Nieger, 2-Halogeno-1,3,2-diazaarsolenes and 2-halogeno-1,3,2-diazastibolenes: Examples for spontaneous E-X bond heterolysis or not?, *Heteroat. Chem.*, 2005, **16**, 327–338.

48 D. Gudat, T. Gans-Eichler and M. Nieger, Synthesis and unprecedented oxidation of a cationic Sb-analogue of an Arduengo's carbene, *Chem. Commun.*, 2004, 2434–2435, DOI: **10.1039/B409657F**.

49 (*a*) CCDC 2495433: Experimental Crystal Structure Determination, 2025, DOI: **10.5517/ccdc.csd.cc2prpv0**; (*b*) CCDC 2495434: Experimental Crystal Structure Determination, 2025, DOI: **10.5517/ccdc.csd.cc2prpw1**.